PHILOSOPHICAL TRANSACTIONS OF THE ROYAL SOCIETY A MATHEMATICAL, PHYSICAL & ENGINEERING SCIENCES

Group-theoretic insights on the vibration of symmetric structures in engineering

Alphose Zingoni

Phil. Trans. R. Soc. A 2014 **372**, 20120037, published 30 December 2013

PHILOSOPHICAL TRANSACTIONS OF THE ROYAL SOCIETY A

rsta.royalsocietypublishing.org

Group-theoretic insights on the vibration of symmetric structures in engineering

Alphose Zingoni

Department of Civil Engineering, University of Cape Town, Rondebosch 7701, Cape Town, South Africa

Research

Cite this article: Zingoni A. 2014 Group-theoretic insights on the vibration of symmetric structures in engineering. *Phil. Trans. R. Soc. A* **372**: 20120037. http://dx.doi.org/10.1098/rsta.2012.0037

One contribution of 14 to a Theo Murphy Meeting Issue 'Rigidity of periodic and symmetric structures in nature and engineering'.

Subject Areas:
structural engineering, civil engineering

Keywords:
group theory, symmetry, structural mechanics, vibration, natural frequency, mode

Author for correspondence:
Alphose Zingoni
e-mail: alphose.zingoni@uct.ac.za

Group theory has been used to study various problems in physics and chemistry for many years. Relatively recently, applications have emerged in engineering, where problems of the vibration, bifurcation and stability of systems exhibiting symmetry have been studied. From an engineering perspective, the main attraction of group-theoretic methods has been their potential to reduce computational effort in the analysis of large-scale problems. In this paper, we focus on vibration problems in structural mechanics and reveal some of the insights and qualitative benefits that group theory affords. These include an appreciation of all the possible symmetries of modes of vibration, the prediction of the number of modes of a given symmetry type, the identification of modes associated with the same frequencies, the prediction of nodal lines and stationary points of a vibrating system, and the untangling of clustered frequencies.

1. Introduction

An object or a system is said to exhibit symmetry if it can be turned into one or more new configurations physically indistinguishable from the initial configuration through the application of one or more symmetry operations, such as reflections in planes, rotations about axes or inversions about some centre. For many years, group theory has provided the mathematical tool for studying problems involving symmetry in physics and chemistry, notably within areas such as quantum mechanics, molecular chemistry and crystallography [1–4].

The last 30 years have also seen applications of group theory finding their way into various areas of engineering mechanics. Bifurcation phenomena in engineering systems have been fruitfully studied using group theory [5–8]. Group theory has also been applied

Royal Society Publishing

to simplify problems of the vibration of a variety of engineering structures [9–17] as well as of the statics and kinematics of skeletal systems encompassing space trusses and frames [18–22]. More recently, applications have been extended to numerical methods, such as finite elements and finite differences [23–28]. Symmetry is central to all group-theoretic formulations, and procedures for the automatic recognition of symmetry groups are now being developed [29]. Progress on applications of group theory within solid and structural mechanics over the past 30 years may be seen in a recent survey [30].

The common feature of all group-theoretic methods is the decomposition of the vector space of the problem into a number of smaller subspaces spanned by symmetry-adapted variables as basis vectors. If the formulation involves a stiffness matrix, this is rendered into block-diagonal form by the procedure, each block being associated with a particular subspace of the problem. The subspace problems (each of dimension a fraction of that of the original problem) are solved-for independently of each other, thus achieving considerable simplification of the problem and overall reductions in computational effort.

Not only does the group-theoretic approach reduce computational effort, but it can also give other computational benefits. With regard to group-theoretic studies in structural mechanics, bifurcation problems have probably received the most attention. In this area, several instances of the qualitative benefits of group-theoretic analyses have been reported in the literature. In studying the global bifurcation behaviour of symmetric structures, computational problems are often encountered owing to the existence of multiple critical points, where two or more eigenvalues vanish simultaneously [31]. The group-theoretic approach has been found to be naturally suited to untangling the problem and simplifying the extraction of eigenvalues.

An important class of space structures comprises lattice domes, which usually possess a high degree of symmetry and are thus amenable to study using group theory. Structural configurations belonging to the dihedral groups D_n (i.e. groups describing the symmetry of regular polygons) have received particular attention in the past [7,31,32]. Bifurcation patterns of D_n configurations are generally less symmetric than the configurations themselves, bifurcation being a process of 'symmetry breaking'. Thus, one may predict that the patterns will in general retain only part of the original symmetry, represented by the subgroups of D_n (which are lower order dihedral groups) and cyclic groups C_m (whose order m is an integer factor of n).

Ikeda *et al*. [31] have studied the bifurcation behaviour of D_n and C_n symmetric structures, and derived a logical sequence for the symmetry-breaking process of bifurcation. One of their observations is that the number of bifurcation paths for such systems is equal to $2n/m$ (twice the ratio of the order of a group to that of a subgroup). Bifurcation paths can undergo further progressive symmetry-breaking bifurcation until they reach a completely asymmetric pattern C_1, and the collection of such successive bifurcations makes up what they termed a 'hierarchy'.

In studying the global bifurcation problem of symmetric structures, Healey [7] considered the example of a lattice dome with hexagonal symmetry and showed that a reduced problem (as yielded by the group-theoretic formulation) does not possess a singularity at a (symmetry-breaking) bifurcation point of the full problem, circumventing the usual numerical problems near bifurcation points (the possibility of 'straying' of solutions onto the wrong paths).

In tackling the problem of the postbuckling behaviour of an axially compressed cylindrical shell, Wohlever & Healey [33] note that the main computational difficulty is the severe ill-conditioning of the tangent-stiffness matrix, owing to the closely spaced symmetry-breaking bifurcation points on the primary axisymmetric solution branch. They then employ group theory to circumvent this ill-conditioning, by using symmetry-adapted variables (reflecting the symmetry of the various solution paths, and hence also referred to as 'symmetry modes') as the basis vectors for the independent subspaces of the original vector space of the problem.

Qualitative considerations of the above types have allowed useful insights to be gained in advance of actual numerical computations. In this paper, we explore further qualitative benefits and insights of the group-theoretic approach as applied to vibration analysis. These benefits will be brought out via a number of examples. Before going into these considerations, it is useful to start off with some definitions and an outline of basic concepts.

2. Symmetry groups and subspace operators

A set of elements $\{a, b, c, \ldots, g, \ldots\}$ constitute a group G with respect to a binary operation (for example, multiplication) if the following axioms are satisfied [1]:

— the product c of any two elements a and b of the group, denoted by $c = ab$, must be a unique element which also belongs to the group;
— among the elements of G, there must exist an identity element e which, when multiplied with any element a of the group, leaves the element unchanged: $ea = ae = a$;
— for every element a of G, there must exist another element d also belonging to the group G, such that $ad = da = e$; d is referred to as the inverse of a and denoted by a^{-1}; and
— the order of the multiplication of three or more elements of G does not affect the result (that is, multiplication is associative): $(ab)c = a(bc)$.

When all elements of G are symmetry operations, then the group G is called a *symmetry group*. Symmetry operations are transformations which bring an object into coincidence with itself and leave it indistinguishable from its original configuration. For finite objects, symmetry operations are typically of the following types:

— reflections in planes of symmetry, denoted by σ_l, where l is the plane of symmetry;
— rotations about an axis of symmetry, denoted by C_n, if the angle of rotation is $2\pi/n$; and
— rotation–reflections, denoted by S_n; these represent a rotation through an angle $2\pi/n$, combined with a reflection in the plane perpendicular to the axis of rotation.

According to representation theory [1], idempotents $P^{(i)}$ of a symmetry group G are linear combinations of its elements satisfying the relation $P^{(i)}P^{(i)} = P^{(i)}$ and $P^{(i)}P^{(j)} = 0$ if $i \neq j$. By operating on vectors of the space Q, an idempotent $P^{(i)}$ nullifies every vector which does not belong to the subspace $S^{(i)}$ and selects all vectors belonging to the subspace $S^{(i)}$ (which will all have a definite symmetry-type characteristic of the subspace). It therefore acts as a *projection operator* [1] of the subspace $S^{(i)}$. When applied upon the functions $\phi_1, \phi_2, \ldots, \phi_n$ of an n-dimensional physical problem, idempotents generate the *symmetry-adapted functions* for their respective subspaces, enabling basis vectors for the various subspaces to be written down. As examples, idempotents of the groups C_{2v}, C_{3v}, C_{4v} and C_{6v}, describing the symmetry properties of a rectangle, an equilateral triangle, a square and a regular hexagon, respectively, are as follows [11,14,18]:

Group C_{2v}

$$P^{(1)} = \tfrac{1}{4}(e + C_2 + \sigma_x + \sigma_y), \tag{2.1a}$$

$$P^{(2)} = \tfrac{1}{4}(e + C_2 - \sigma_x - \sigma_y), \tag{2.1b}$$

$$P^{(3)} = \tfrac{1}{4}(e - C_2 + \sigma_x - \sigma_y) \tag{2.1c}$$

and

$$P^{(4)} = \tfrac{1}{4}(e - C_2 - \sigma_x + \sigma_y). \tag{2.1d}$$

Group C_{3v}

$$P^{(1)} = \tfrac{1}{6}(e + C_3 + C_3^{-1} + \sigma_1 + \sigma_2 + \sigma_3), \tag{2.2a}$$

$$P^{(2)} = \tfrac{1}{6}(e + C_3 + C_3^{-1} - \sigma_1 - \sigma_2 - \sigma_3) \tag{2.2b}$$

and

$$P^{(3)} = \tfrac{1}{3}(2e - C_3 - C_3^{-1}). \tag{2.2c}$$

Group C_{4v}

$$P^{(1)} = \tfrac{1}{8}(e + C_4 + C_4^{-1} + C_2 + \sigma_x + \sigma_y + \sigma_1 + \sigma_2), \tag{2.3a}$$

$$P^{(2)} = \tfrac{1}{8}(e + C_4 + C_4^{-1} + C_2 - \sigma_x - \sigma_y - \sigma_1 - \sigma_2), \tag{2.3b}$$

$$P^{(3)} = \tfrac{1}{8}(e - C_4 - C_4^{-1} + C_2 + \sigma_x + \sigma_y - \sigma_1 - \sigma_2), \tag{2.3c}$$

$$P^{(4)} = \tfrac{1}{8}(e - C_4 - C_4^{-1} + C_2 - \sigma_x - \sigma_y + \sigma_1 + \sigma_2) \tag{2.3d}$$

and

$$P^{(5)} = \tfrac{1}{2}(e - C_2) = P^{(5,1)} + P^{(5,2)}, \tag{2.3e}$$

where for equation (2.3*e*) either of equations (2.4) or (2.5) below hold

$$P^{(5,1)} = \tfrac{1}{4}(e - C_2 + \sigma_1 - \sigma_2); \quad P^{(5,2)} = \tfrac{1}{4}(e - C_2 - \sigma_1 + \sigma_2) \tag{2.4}$$

or

$$P^{(5,1)} = \tfrac{1}{4}(e - C_2 + \sigma_x - \sigma_y); \quad P^{(5,2)} = \tfrac{1}{4}(e - C_2 - \sigma_x + \sigma_y). \tag{2.5}$$

Group C_{6v}

$$P^{(1)} = \tfrac{1}{12}(e + C_6 + C_6^{-1} + C_3 + C_3^{-1} + C_2 + \sigma_a + \sigma_b + \sigma_c + \sigma_1 + \sigma_2 + \sigma_3), \tag{2.6a}$$

$$P^{(2)} = \tfrac{1}{12}(e + C_6 + C_6^{-1} + C_3 + C_3^{-1} + C_2 - \sigma_a - \sigma_b - \sigma_c - \sigma_1 - \sigma_2 - \sigma_3), \tag{2.6b}$$

$$P^{(3)} = \tfrac{1}{12}(e - C_6 - C_6^{-1} + C_3 + C_3^{-1} - C_2 + \sigma_a + \sigma_b + \sigma_c - \sigma_1 - \sigma_2 - \sigma_3), \tag{2.6c}$$

$$P^{(4)} = \tfrac{1}{12}(e - C_6 - C_6^{-1} + C_3 + C_3^{-1} - C_2 - \sigma_a - \sigma_b - \sigma_c + \sigma_1 + \sigma_2 + \sigma_3), \tag{2.6d}$$

$$P^{(5)} = \tfrac{1}{6}(2e + C_6 + C_6^{-1} - C_3 - C_3^{-1} - 2C_2) \tag{2.6e}$$

and

$$P^{(6)} = \tfrac{1}{6}(2e - C_6 - C_6^{-1} - C_3 - C_3^{-1} + 2C_2). \tag{2.6f}$$

In the above expressions, e denotes the identity element, while C_n denotes a rotation about the primary axis of symmetry (assumed perpendicular to the plane of the polygon and passing through the centre of symmetry) through an angle of $2\pi/n$. Throughout this paper, $\{\sigma_x, \sigma_y\}$ for rectangular (including square) configurations denote reflections in planes containing the x and y coordinate axes, respectively (these are taken to pass through the mid-sides of the rectangle), $\{\sigma_1, \sigma_2\}$ for square configurations denote reflections in the planes of the diagonals, $\{\sigma_1, \sigma_2, \sigma_3\}$ for triangular configurations denote reflections in the three planes of symmetry of the equilateral triangle (these pass through a vertex and the opposite mid-side of the triangle), $\{\sigma_1, \sigma_2, \sigma_3\}$ for hexagonal configurations denote reflections in the three planes of symmetry that pass through opposite vertices of the hexagon, while $\{\sigma_a, \sigma_b, \sigma_c\}$ denote reflections in the three planes of symmetry that bisect opposite sides of the hexagon.

For the symmetry group C_{4v}, the conceptual splitting of idempotent $P^{(5)}$ of subspace $S^{(5)}$ into two independent operators $P^{(5,1)}$ and $P^{(5,2)}$ is not a standard result from representation theory, but a means for decomposing the subspace $S^{(5)}$ into two identical subspaces $S^{(5,1)}$ and $S^{(5,2)}$ which are spanned by physically indistinguishable symmetry-adapted functions. For the two independent operators $P^{(5,1)}$ and $P^{(5,2)}$, we may adopt the pair given as equations (2.4) or (2.5), but not both. Adopting either pair, it may readily be seen that $P^{(5,1)}P^{(5,1)} = P^{(5,1)}$ and $P^{(5,2)}P^{(5,2)} = P^{(5,2)}$. Moreover, and more importantly, it is established that $P^{(5,1)}P^{(5,2)} = 0$ (the operators are mutually orthogonal) and $P^{(5,1)}P^{(j)} = P^{(5,2)}P^{(j)} = 0$ for $j = \{1, 2, 3, 4\}$ (each operator is also orthogonal to the idempotents of the first four subspaces of the group).

A symmetry group G with k idempotents $\{P^{(1)}, P^{(2)}, \ldots, P^{(k)}\}$ generally decomposes an n-dimensional problem (i.e. one with n degrees of freedom in the case of vibration problems) into k corresponding independent subspaces $\{S^{(1)}, S^{(2)}, \ldots, S^{(k)}\}$, each $S^{(i)}$ $(i = 1, 2, \ldots, k)$ spanned by a number r_i of symmetry-adapted functions that is typically small in comparison with n, as $r_1 + r_2 + \ldots + r_k = n$. To illustrate the group-theoretic computational steps for obtaining actual frequencies and mode shapes, and to show the insights that are gained through such an approach, we consider a number of vibration problems: spring–mass systems [16], cable nets [11], layered space grids [14] and continuum plates [28].

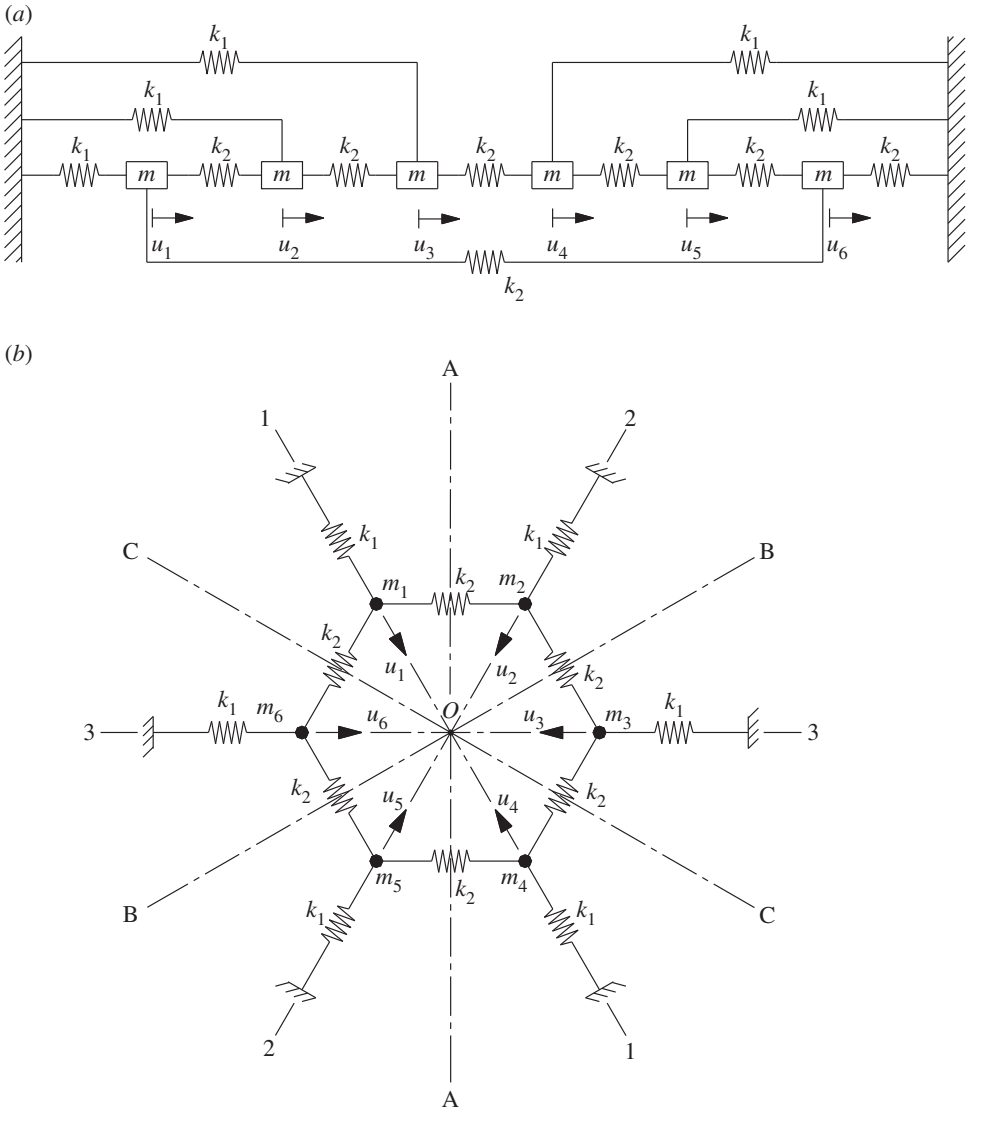

Figure 1. Spring–mass system with six degrees of freedom: (*a*) actual configuration and (*b*) equivalent symmetric system.

3. Spring–mass systems

A spring–mass system with six degrees of freedom is shown in figure 1*a*. The masses are all equal ($m_i = m$ for $i = 1, 2, \ldots, 6$). The *topologically* equivalent symmetric system is shown in figure 1*b*. The systems of figure 1*a*,*b* are equivalent in the sense of having the same mass connectivities, and not in the sense of having the same static and dynamic characteristics, such as stiffness and natural frequencies. Thus, any given mass m_i ($i = 1, 2, \ldots, 6$) in figure 1*b* is connected to the same values of adjacent masses and same type of adjacent support, via the same values of spring stiffnesses, as its counterpart in figure 1*a*. The symmetric system in figure 1*b* has a centre of symmetry O, and the symmetry elements: e (identity); C_6 and C_6^{-1} (clockwise and anticlockwise rotations of $2\pi/6$ about O); C_3 and C_3^{-1} (clockwise and anticlockwise rotations of $2\pi/3$ about O); C_2 (rotation of π about O); and $\sigma_a, \sigma_b, \sigma_c, \sigma_1, \sigma_2$ and σ_3 (reflections in the vertical planes as labelled in the figure). Note that for the reflection planes labelled as A, B and C in the figure, the corresponding symmetry elements are denoted by lower case subscripts a, b and c. The configuration therefore

belongs to the symmetry group C_{6v} of order 12. The positive direction of the rectilinear freedoms u_1, u_2, u_3, u_4, u_5 and u_6 of the original system (figure 1*a*) maps into the direction towards the centre in the equivalent symmetric system (figure 1*b*).

If we apply the first idempotent $P^{(1)}$ of the symmetry group C_{6v} (this is given by equation (2.6*a*)) to all the six freedoms u_i $(i = 1, 2, \ldots, 6)$ of the configuration of figure 1*b*, we obtain six symmetry-adapted freedoms for the first subspace, not all of which are independent. To illustrate this, consider the application of $P^{(1)}$ to the first freedom u_1, the relevant steps being as follows:

$$\begin{aligned} P^{(1)}u_1 &= \tfrac{1}{12}(e + C_6 + C_6^{-1} + C_3 + C_3^{-1} + C_2 + \sigma_a + \sigma_b + \sigma_c + \sigma_1 + \sigma_2 + \sigma_3)u_1 \\ &= \tfrac{1}{12}(u_1 + u_2 + u_6 + u_3 + u_5 + u_4 + u_2 + u_4 + u_6 + u_1 + u_3 + u_5) \\ &= \tfrac{1}{6}(u_1 + u_2 + u_3 + u_4 + u_5 + u_6). \end{aligned}$$

This result (on the last line) is the same result we get by applying $P^{(1)}$ to u_2, u_3, u_4, u_5 and u_6. Thus, in this case, there is only one linearly independent symmetry-adapted freedom.

We repeat the procedure for all subspaces, using the correct idempotent for the subspace in question (that is, we use $P^{(i)}$ for subspace $S^{(i)}$, $i = 1, 2, \ldots, 6$). Selecting a set of linearly independent symmetry-adapted freedoms as the basis vectors for the subspace, we obtain the following results for the basis vectors of the subspaces (note that common multipliers, for example 1/6, are not important and have been dropped off):

Subspace $S^{(1)}$

$$\Phi^{(1)} = u_1 + u_2 + u_3 + u_4 + u_5 + u_6. \tag{3.1}$$

Subspace $S^{(4)}$

$$\Phi^{(4)} = u_1 - u_2 + u_3 - u_4 + u_5 - u_6. \tag{3.2}$$

Subspace $S^{(5)}$

$$\Phi_1^{(5)} = u_1 + \tfrac{1}{2}u_2 - \tfrac{1}{2}u_3 - u_4 - \tfrac{1}{2}u_5 + \tfrac{1}{2}u_6 \tag{3.3a}$$

and

$$\Phi_2^{(5)} = \tfrac{1}{2}u_1 + u_2 + \tfrac{1}{2}u_3 - \tfrac{1}{2}u_4 - u_5 - \tfrac{1}{2}u_6. \tag{3.3b}$$

Subspace $S^{(6)}$

$$\Phi_1^{(6)} = u_1 - \tfrac{1}{2}u_2 - \tfrac{1}{2}u_3 + u_4 - \tfrac{1}{2}u_5 - \tfrac{1}{2}u_6 \tag{3.4a}$$

and

$$\Phi_2^{(6)} = -\tfrac{1}{2}u_1 + u_2 - \tfrac{1}{2}u_3 - \tfrac{1}{2}u_4 + u_5 - \tfrac{1}{2}u_6. \tag{3.4b}$$

From the above results, we see that subspaces $S^{(1)}$ and $S^{(4)}$ are one dimensional (that is, spanned by one basis vector each), subspaces $S^{(5)}$ and $S^{(6)}$ are two dimensional, while subspaces $S^{(2)}$ and $S^{(3)}$ are null spaces. We have thus decomposed the original six-dimensional vector space of the problem into four independent subspaces of smaller dimensions, spanned by the above sets of symmetry-adapted freedoms. Each subspace is associated with a specific symmetry type.

For subspace $S^{(1)}$, if we apply a unit positive displacement simultaneously on each mass m_i $(i = 1, 2, \ldots, 6)$ in accordance with the coordinates of the basis vector $\Phi^{(1)}$ (equation (3.1)) as shown in figure 2*a*, we see that the ensuing restoring force on each mass is equal to k_1. Thus,

$$\mathbf{K}^{(1)} = k_{11}^{(1)} = [k_1] \quad \text{and} \quad \mathbf{M}^{(1)} = m_{11}^{(1)} = [m]. \tag{3.5}$$

This leads to the first-degree characteristic equation

$$k_1 - \omega^2 m = 0 \tag{3.6}$$

and the solution

$$\omega^2 = \frac{k_1}{m}. \tag{3.7}$$

For subspace $S^{(4)}$, applying a unit displacement simultaneously on each mass, in accordance with the coordinates of the basis vector $\Phi^{(4)}$ (equation (3.2)) as shown in figure 2*b*, results in a restoring

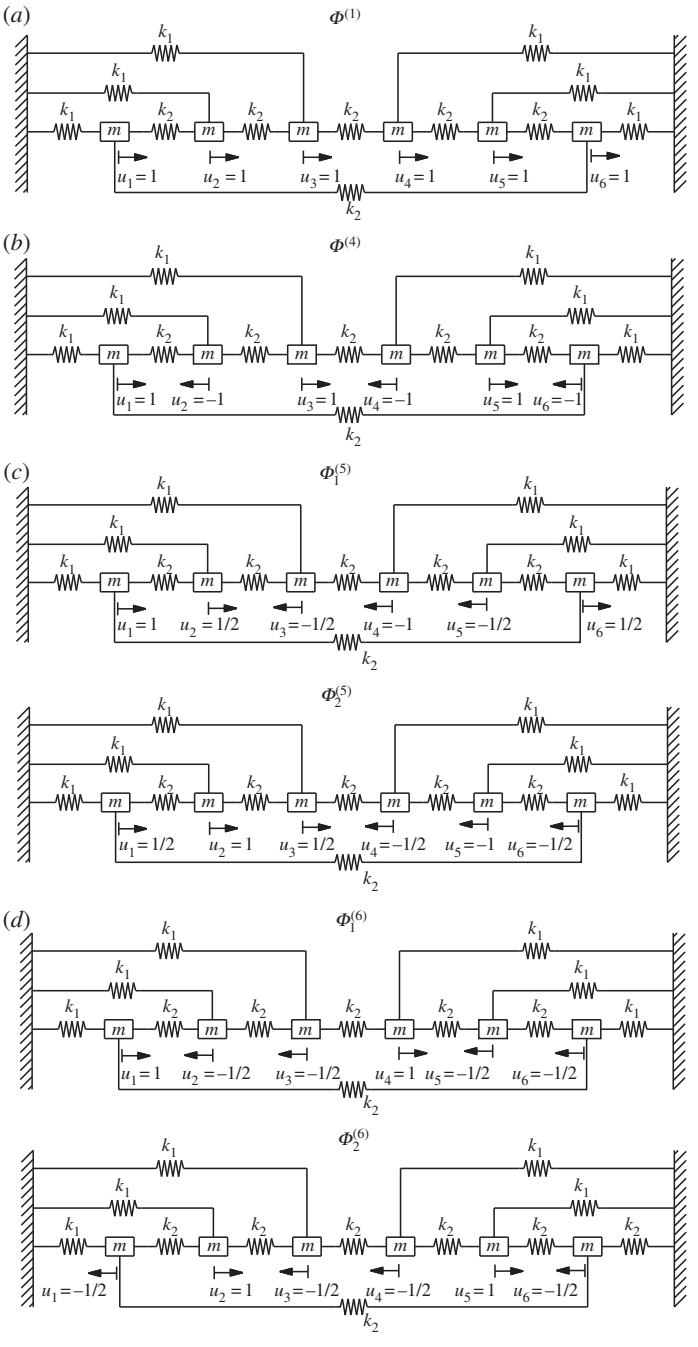

Figure 2. Spring–mass system: application of displacement components of the basis vectors: (*a*) subspace $S^{(1)}$; (*b*) subspace $S^{(4)}$; (*c*) subspace $S^{(5)}$; and (*d*) subspace $S^{(6)}$.

force of $(k_1 + 4k_2)$ on each mass. Thus,

$$\mathbf{K}^{(4)} = k_{11}^{(4)} = [k_1 + 4k_2] \quad \text{and} \quad \mathbf{M}^{(4)} = m_{11}^{(4)} = [m], \tag{3.8}$$

which leads to the first-degree characteristic equation

$$(k_1 + 4k_2) - \omega^2 m = 0 \tag{3.9}$$

Table 1. Restoring forces owing to the application of the components of $\Phi_1^{(5)}$ and $\Phi_2^{(5)}$ for the spring–mass system.

	$\Phi_1^{(5)}$		$\Phi_2^{(5)}$	
mass	displacement	restoring force	displacement	restoring force
$m_1 = m$	$u_1 = +1.0$	$+1.0(k_1 + k_2)$	$u_1 = +0.5$	$+0.5(k_1 + k_2)$
$m_2 = m$	$u_2 = +0.5$	$+0.5(k_1 + k_2)$	$u_2 = +1.0$	$+1.0(k_1 + k_2)$
$m_3 = m$	$u_3 = -0.5$	$-0.5(k_1 + k_2)$	$u_3 = +0.5$	$+0.5(k_1 + k_2)$
$m_4 = m$	$u_4 = -1.0$	$-1.0(k_1 + k_2)$	$u_4 = -0.5$	$-0.5(k_1 + k_2)$
$m_5 = m$	$u_5 = -0.5$	$-0.5(k_1 + k_2)$	$u_5 = -1.0$	$-1.0(k_1 + k_2)$
$m_6 = m$	$u_6 = +0.5$	$+0.5(k_1 + k_2)$	$u_6 = -0.5$	$-0.5(k_1 + k_2)$

Table 2. Restoring forces owing to the application of the components of $\Phi_1^{(6)}$ and $\Phi_2^{(6)}$ for the spring–mass system.

	$\Phi_1^{(6)}$		$\Phi_2^{(6)}$	
mass	displacement	restoring force	displacement	restoring force
$m_1 = m$	$u_1 = +1.0$	$+1.0(k_1 + 3k_2)$	$u_1 = -0.5$	$-0.5(k_1 + 3k_2)$
$m_2 = m$	$u_2 = -0.5$	$-0.5(k_1 + 3k_2)$	$u_2 = +1.0$	$+1.0(k_1 + 3k_2)$
$m_3 = m$	$u_3 = -0.5$	$-0.5(k_1 + 3k_2)$	$u_3 = -0.5$	$-0.5(k_1 + 3k_2)$
$m_4 = m$	$u_4 = +1.0$	$+1.0(k_1 + 3k_2)$	$u_4 = -0.5$	$-0.5(k_1 + 3k_2)$
$m_5 = m$	$u_5 = -0.5$	$-0.5(k_1 + 3k_2)$	$u_5 = +1.0$	$+1.0(k_1 + 3k_2)$
$m_6 = m$	$u_6 = -0.5$	$-0.5(k_1 + 3k_2)$	$u_6 = -0.5$	$-0.5(k_1 + 3k_2)$

and the solution

$$\omega^2 = \frac{k_1 + 4k_2}{m}. \tag{3.10}$$

For subspace $S^{(5)}$, the restoring forces on each of the masses m_i $(i = 1, 2, \ldots, 6)$, resulting from the application of the displacement components making up the basis vectors $\Phi_1^{(5)}$ and $\Phi_2^{(5)}$ (equations (3.3)) as shown in figure 2*c*, are summarized in table 1. Similarly for subspace $S^{(6)}$, the restoring forces on each of the masses m_i, resulting from the application of the displacement components making up the basis vectors $\Phi_1^{(6)}$ and $\Phi_2^{(6)}$ (equations (3.4)) as shown in figure 2*d*, are summarized in table 2.

Consider subspace $S^{(5)}$ first. For the application of either $\Phi_1^{(5)}$ or $\Phi_2^{(5)}$, it is noted (from table 1) that all restoring forces are proportional to the u value prescribed to the mass in question. Taking unit positive value of u (i.e. $u = +1$), the corresponding restoring force is $(k_1 + k_2)$ in either case. Therefore,

$$\left.\begin{aligned} k_{11}^{(5)} = (k_1 + k_2); \quad k_{12}^{(5)} = 0 \\ k_{21}^{(5)} = 0; \quad k_{22}^{(5)} = (k_1 + k_2). \end{aligned}\right\} \tag{3.11}$$

The symmetry-adapted stiffness matrix $\mathbf{K}^{(5)}$ is therefore (corresponding mass matrix also given)

$$\mathbf{K}^{(5)} = \begin{bmatrix} (k_1 + k_2) & 0 \\ 0 & (k_1 + k_2) \end{bmatrix} \quad \text{and} \quad \mathbf{M}^{(5)} = \begin{bmatrix} m & 0 \\ 0 & m \end{bmatrix}. \tag{3.12}$$

This leads to two uncoupled first-degree characteristic equations

$$(k_1 + k_2) - \omega^2 m = 0 \quad \text{(twice)}, \tag{3.13}$$

giving the solutions

$$(\omega^2)_1^{(5)} = (\omega^2)_2^{(5)} = \frac{k_1 + k_2}{m}. \tag{3.14}$$

Similarly for subspace $S^{(6)}$, for the application of either $\Phi_1^{(6)}$ or $\Phi_2^{(6)}$, it is noted (from table 2) that all restoring forces are also proportional to the u value prescribed to the mass in question. Taking unit positive value of u (i.e. $u = +1$), the corresponding restoring force is $(k_1 + 3k_2)$ in either case. Hence,

$$\left.\begin{aligned} k_{11}^{(6)} &= (k_1 + 3k_2); \quad k_{12}^{(6)} = 0 \\ k_{21}^{(6)} &= 0; \quad k_{22}^{(6)} = (k_1 + 3k_2). \end{aligned}\right\} \tag{3.15}$$

The symmetry-adapted stiffness matrix $\mathbf{K}^{(6)}$ is therefore (corresponding mass matrix also given)

$$\mathbf{K}^{(6)} = \begin{bmatrix} (k_1 + 3k_2) & 0 \\ 0 & (k_1 + 3k_2) \end{bmatrix} \quad \text{and} \quad \mathbf{M}^{(6)} = \begin{bmatrix} m & 0 \\ 0 & m \end{bmatrix}, \tag{3.16}$$

leading to two uncoupled first-degree characteristic equations

$$(k_1 + 3k_2) - \omega^2 m = 0 \quad \text{(twice)}, \tag{3.17}$$

with the solutions

$$(\omega^2)_1^{(6)} = (\omega^2)_2^{(6)} = \frac{k_1 + 3k_2}{m}. \tag{3.18}$$

In summary, subspaces $S^{(1)}$ and $S^{(4)}$ yielded one eigenvalue each; subspaces $S^{(5)}$ and $S^{(6)}$ each yielded two equal eigenvalues (doubly repeating roots). Putting the solutions together, the six natural circular frequencies of the original system (in ascending order) are as follows:

$$\omega_1^2 = \frac{k_1}{m}; \quad \omega_2^2 = \omega_3^2 = \frac{k_1 + k_2}{m}; \quad \omega_4^2 = \omega_5^2 = \frac{k_1 + 3k_2}{m}; \quad \text{and} \quad \omega_6^2 = \frac{k_1 + 4k_2}{m}. \tag{3.19}$$

Instead of having to expand a 6×6 determinant and solve a sixth-degree characteristic polynomial as yielded by conventional considerations, the group-theoretic approach required the solution of only four separate *first-degree* characteristic equations, yielding all six eigenvalues (two distinct roots and two pairs of repeated roots) of the original problem. Here, we see that the computational effort of the group-theoretic procedure is less than 10% of that associated with conventional analysis. Spring–mass models of other symmetry groups may be seen in [16].

4. Cable nets

To illustrate the flexibility formulation of the vibration problem, let us consider a three-dimensional but shallow cable net formed by two families of highly tensioned cables intersecting perpendicularly on the xy horizontal projection (figure 3). The net has 16 nodes or cable intersections, numbered as shown in the figure. This particular example is taken from [11]. Clearly, the configuration has the symmetry of a square, and therefore belongs to the symmetry group C_{4v}. In this example, the horizontal spacing between cables is taken as constant and equal to a. The horizontal component of the cable prestress force, denoted as T_1 or T_2 in the figure, is assumed to be constant over the entire length of the cable. The T_1 and T_2 pattern (that is, the prestressing pattern) conforms to the C_{4v} symmetry of the cable layout. We require to evaluate the free vibration response of the system, where the degrees of freedom are the small transverse motions of masses lumped at the cable intersections.

(a) Symmetry-adapted functions

The 16-dimensional vector space of the problem can be decomposed into six independent subspaces spanned by symmetry-adapted variables. To obtain the symmetry-adapted functions for a given subspace $S^{(i)}$, we apply the corresponding idempotent $P^{(i)}$ as an operator on each function ϕ_j $(j = 1, 2, \ldots, 16)$ of the problem, and then select a linearly independent set of the

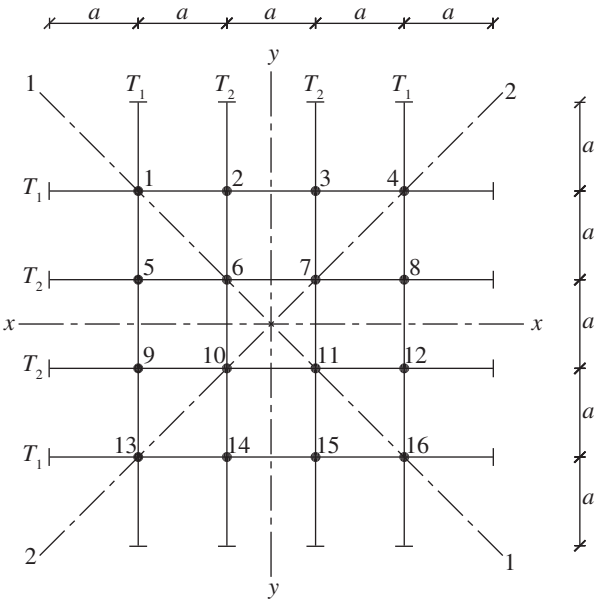

Figure 3. Horizontal projection of cable net showing cable prestress forces.

symmetry-adapted functions as the basis vectors spanning the subspace. For the present problem, the relevant $P^{(i)}$ are given by equations (2.3*a–d*) and equations (2.4). The results are:

Subspace $S^{(1)}$

$$\Phi_1^{(1)} = \phi_1 + \phi_4 + \phi_{13} + \phi_{16}, \tag{4.1a}$$

$$\Phi_2^{(1)} = \phi_2 + \phi_3 + \phi_5 + \phi_8 + \phi_9 + \phi_{12} + \phi_{14} + \phi_{15} \tag{4.1b}$$

and

$$\Phi_3^{(1)} = \phi_6 + \phi_7 + \phi_{10} + \phi_{11}. \tag{4.1c}$$

Subspace $S^{(2)}$

$$\Phi_1^{(2)} = \phi_2 - \phi_3 - \phi_5 + \phi_8 + \phi_9 - \phi_{12} - \phi_{14} + \phi_{15}. \tag{4.2}$$

Subspace $S^{(3)}$

$$\Phi_1^{(3)} = \phi_2 + \phi_3 - \phi_5 - \phi_8 - \phi_9 - \phi_{12} + \phi_{14} + \phi_{15}. \tag{4.3}$$

Subspace $S^{(4)}$

$$\Phi_1^{(4)} = \phi_1 - \phi_4 - \phi_{13} + \phi_{16}, \tag{4.4a}$$

$$\Phi_2^{(4)} = \phi_2 - \phi_3 + \phi_5 - \phi_8 - \phi_9 + \phi_{12} - \phi_{14} + \phi_{15} \tag{4.4b}$$

and

$$\Phi_3^{(4)} = \phi_6 - \phi_7 - \phi_{10} + \phi_{11}. \tag{4.4c}$$

Subspace $S^{(5,1)}$

$$\Phi_1^{(5,1)} = \Phi_1^{(5)} = \phi_1 - \phi_{16}, \tag{4.5a}$$

$$\Phi_2^{(5,1)} = \Phi_6^{(5)} = \phi_6 - \phi_{11}, \tag{4.5b}$$

$$\Phi_3^{(5,1)} = \Phi_3^{(5)} - \Phi_8^{(5)} = \phi_3 - \phi_8 + \phi_9 - \phi_{14} \tag{4.5c}$$

and

$$\Phi_4^{(5,1)} = \Phi_2^{(5)} + \Phi_5^{(5)} = \phi_2 + \phi_5 - \phi_{12} - \phi_{15}. \tag{4.5d}$$

Subspace $S^{(5,2)}$

$$\Phi_1^{(5,2)} = \Phi_4^{(5)} = \phi_4 - \phi_{13}, \tag{4.6a}$$

$$\Phi_2^{(5,2)} = \Phi_7^{(5)} = \phi_7 - \phi_{10}, \tag{4.6b}$$

$$\Phi_3^{(5,2)} = \Phi_3^{(5)} + \Phi_8^{(5)} = \phi_3 + \phi_8 - \phi_9 - \phi_{14} \tag{4.6c}$$

and

$$\Phi_4^{(5,2)} = \Phi_2^{(5)} - \Phi_5^{(5)} = \phi_2 - \phi_5 + \phi_{12} - \phi_{15}. \tag{4.6d}$$

Thus, the 16-dimensional vector space of the original problem is decomposed into a total of six r-dimensional subspaces, where $r = \{3, 1, 1, 3, 4, 4\}$ for subspaces $S^{(1)}$, $S^{(2)}$, $S^{(3)}$, $S^{(4)}$, $S^{(5,1)}$ and $S^{(5,2)}$, respectively. Computations need only be performed in these reduced spaces.

(b) Symmetry-adapted flexibility matrices

For each subspace of the problem, we apply unit vertical forces upon the cable-net nodes in accordance with the coordinates of the respective basis vectors, as shown in the diagrams of figure 4. For a given subspace, each vector Φ_i has been plotted on a separate diagram, for clarity. The symbols $\otimes$ and $\odot$ in these diagrams denote positive (i.e. downward) and negative (i.e. upward) unit forces, respectively. To avoid clutter, the numbering of the nodes is not shown; the diagrams have exactly the same orientation as in figure 3. For the same reason, the Φ_i labels are shown without the subspace superscript; the subspace is indicated in the figure caption.

If all the r basis-vector plots of a given subspace (shown separately in figure 4) are superimposed on one diagram, any nodes that remain unaffected (that is, not associated with any one of the r basis vectors of the subspace) imply *stationary* points. By doing this simple superposition exercise, we find that subspaces $S^{(2)}$ and $S^{(3)}$ are each associated with eight stationary nodes (the points lying on either of the two principal diagonals of the net), whereas subspaces $S^{(5,1)}$ and $S^{(5,2)}$ are each associated with the occurrence of four stationary nodes (the points lying on *one* of the two principal diagonals of the net).

From the plots of figure 4, we may make an important observation. The set of basis vectors for subspace $S^{(5,1)}$ is very similar to that for subspace $S^{(5,2)}$ (compare figure 4*e* and figure 4*f*). For every vector in $S^{(5,1)}$, there is one exactly identical to it in $S^{(5,2)}$, except for orientation. Clearly the physical properties of a physical system, such as natural frequencies and modes of deformation, are not affected by its orientation in space. Therefore, a solution for any required physical properties based on subspace $S^{(5,1)}$ must be identical to that based on subspace $S^{(5,2)}$. These subspaces will yield identical sets of eigenvalues, hence we need only consider one of them. In the present example, subspace $S^{(5,1)}$ will be selected. Thus, eigenvalues which occur as coincident solutions (doubly repeating roots) in the vector space of the original problem are automatically separated via the group-theoretic decomposition.

Let us consider any one of the subspaces of the problem, such a subspace being spanned by r basis vectors. Let us define a_{ij} $(i = 1, 2, \ldots, r; j = 1, 2, \ldots, r)$ as the vertical-displacement magnitude at *any* of the nodes of the basis vector Φ_i, owing to unit vertical forces applied at *all* the nodes of the basis vector Φ_j. The condition of vertical equilibrium at each of the r sets of nodes (corresponding to the r basis vectors of the subspace) leads to r simultaneous equations in the r deflection unknowns $\{a_{1j}, a_{2j}, \ldots, a_{rj}\}$, which may be expressed as

$$\begin{bmatrix} b_{11} & b_{12} & . & b_{1r} \\ b_{21} & b_{22} & . & b_{2r} \\ . & . & . & . \\ b_{r1} & b_{r2} & . & b_{rr} \end{bmatrix} \begin{bmatrix} a_{1j} \\ a_{2j} \\ . \\ a_{rj} \end{bmatrix} = \begin{bmatrix} \delta_{1j} \\ \delta_{2j} \\ . \\ \delta_{rj} \end{bmatrix} \tag{4.7}$$

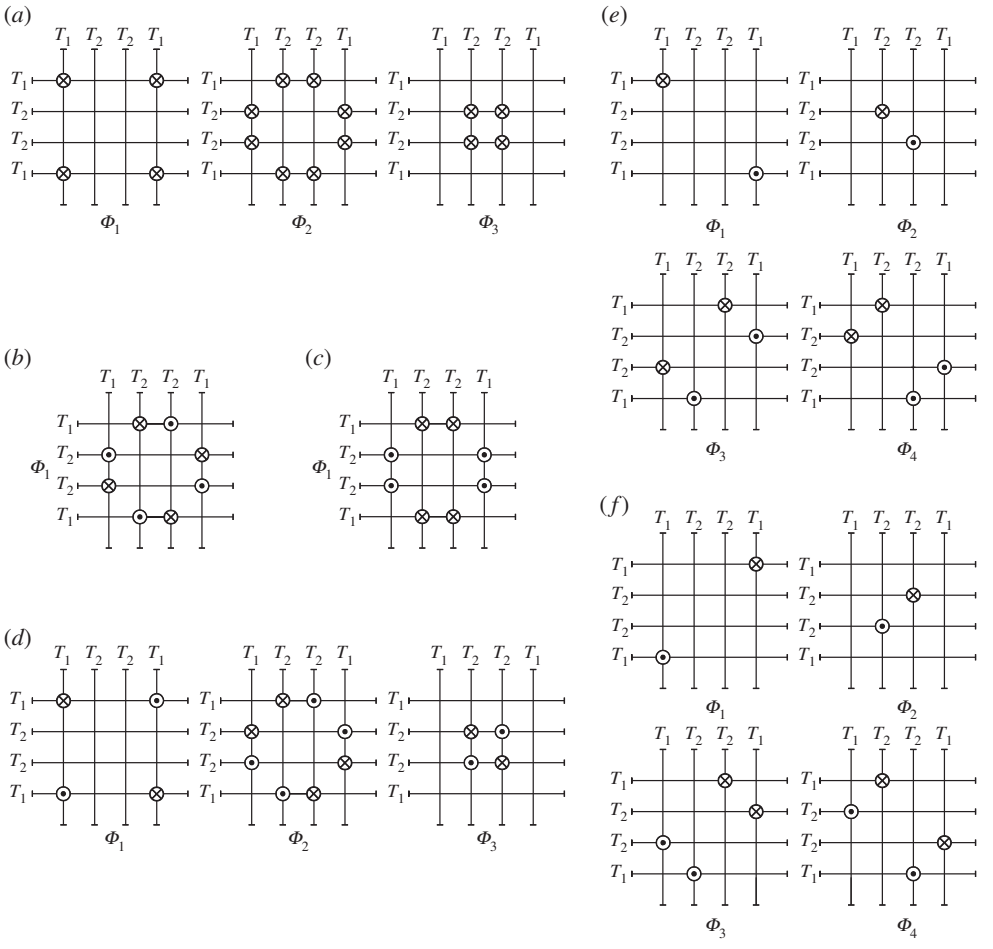

Figure 4. Cable-net system: unit vertical forces applied in accordance with the coordinates of the basis vectors: (*a*) subspace $S^{(1)}$; (*b*) subspace $S^{(2)}$; (*c*) subspace $S^{(3)}$; (*d*) subspace $S^{(4)}$; (*e*) subspace $S^{(5,1)}$; and (*f*) subspace $S^{(5,2)}$.

for $j = 1, 2, \ldots, r$. For the right-hand side, $\delta_{ij} = 1$ if $i = j$, and $\delta_{ij} = 0$ if $i \neq j$. We may write this equation as

$$\mathbf{B}^{(l)}\mathbf{A}_j = \boldsymbol{\delta}_j, \tag{4.8}$$

where $\mathbf{B}^{(l)}$ is an $r \times r$ matrix corresponding to subspace $S^{(l)}$; $\boldsymbol{\delta}_j$ is an $r \times 1$ column vector consisting of a '1' at row j and 'zeros' everywhere else, and $\mathbf{A}_j$ is the $r \times 1$ column vector of the deflections corresponding to the application of unit vertical forces at each of the nodes of Φ_j. These deflections are, by definition, the flexibility coefficients for the subspace. Rearranging equation (4.8) then yields the column vectors $\mathbf{A}_j$ of the flexibility matrix for subspace $S^{(l)}$ (which we can now write as $\mathbf{A}_j^{(l)}$ to denote that they pertain to subspace $S^{(l)}$); when the $\mathbf{A}_j^{(l)}$ are put together, they form the full flexibility matrix $\mathbf{A}^{(l)}$ for subspace $S^{(l)}$,

$$\mathbf{A}_j^{(l)} = [\mathbf{B}^{(l)}]^{-1}\boldsymbol{\delta}_j; \quad j = 1, 2, \ldots, r \tag{4.9}$$

and

$$\mathbf{A}^{(l)} = \left[\mathbf{A}_1^{(l)} \;\middle|\; \mathbf{A}_2^{(l)} \;\middle|\; \ldots \;\middle|\; \mathbf{A}_r^{(l)}\right]. \tag{4.10}$$

The $\mathbf{B}^{(l)}$ matrices for the various subspaces have been obtained as follows:

Subspace $S^{(1)}$

$$\mathbf{B}^{(1)} = \begin{bmatrix} \frac{4T_1}{a} & -\frac{2T_1}{a} & 0 \\ -\frac{T_1}{a} & \frac{T_1+2T_2}{a} & -\frac{T_2}{a} \\ 0 & -\frac{2T_2}{a} & \frac{2T_2}{a} \end{bmatrix}. \tag{4.11a}$$

Subspaces $S^{(2)}$ and $S^{(3)}$

$$\mathbf{B}^{(2)} = \begin{bmatrix} \frac{3T_1+2T_2}{a} \end{bmatrix} \quad \text{and} \quad \mathbf{B}^{(3)} = \begin{bmatrix} \frac{T_1+2T_2}{a} \end{bmatrix}. \tag{4.11b,c}$$

Subspace $S^{(4)}$

$$\mathbf{B}^{(4)} = \begin{bmatrix} \frac{4T_1}{a} & -\frac{2T_1}{a} & 0 \\ -\frac{T_1}{a} & \frac{3T_1+2T_2}{a} & -\frac{T_2}{a} \\ 0 & -\frac{2T_2}{a} & \frac{6T_2}{a} \end{bmatrix}. \tag{4.11d}$$

Subspace $S^{(5,1)}$

$$\mathbf{B}^{(5,1)} = \begin{bmatrix} \frac{4T_1}{a} & 0 & 0 & -\frac{2T_1}{a} \\ 0 & \frac{4T_2}{a} & 0 & -\frac{2T_2}{a} \\ 0 & 0 & \frac{2(T_1+T_2)}{a} & -\frac{T_1}{a} \\ -\frac{T_1}{a} & -\frac{T_2}{a} & -\frac{T_1}{a} & \frac{2(T_1+T_2)}{a} \end{bmatrix}. \tag{4.11e}$$

(c) Subspace mass matrices

Let us assign to the cable net a system of concentrated masses positioned at the nodes (such masses may be actual, or lumped parameters of a distributed-mass system). Referring to figure 3, let the values of these masses be m_1 at each position of the nodal set $\{1, 4, 13, 16\}$, m_2 at each position of the nodal set $\{2, 3, 5, 8, 9, 12, 14, 15\}$ and m_3 at each position of the nodal set $\{6, 7, 10, 11\}$. This pattern of masses conforms to the general symmetry of the cable configuration. The diagonal mass matrix $\mathbf{M}^{(i)}$ for a given subspace $S^{(i)}$ consists of non-zero diagonal elements m_{ii} $(i = 1, 2, \ldots, r)$, which are the values of the mass at any of the nodes of basis vector Φ_i. Thus, the mass matrices for the various subspaces of our problem are as follows:

$$\mathbf{M}^{(1)} = \mathbf{M}^{(4)} = \begin{bmatrix} m_1 & 0 & 0 \\ 0 & m_2 & 0 \\ 0 & 0 & m_3 \end{bmatrix}; \ \mathbf{M}^{(2)} = \mathbf{M}^{(3)} = [m_2] \tag{4.12a,b}$$

$$\mathbf{M}^{(5,1)} = \mathbf{M}^{(5,2)} = \begin{bmatrix} m_1 & 0 & 0 & 0 \\ 0 & m_3 & 0 & 0 \\ 0 & 0 & m_2 & 0 \\ 0 & 0 & 0 & m_2 \end{bmatrix}. \tag{4.12c}$$

(d) Eigenvalues

The system eigenvalues λ ($=1/\omega^2$, where ω is a natural circular frequency of the system) are obtained separately for each subspace, from the well-known vanishing condition

$$|\mathbf{A} - \lambda \mathbf{M}^{-1}| = 0. \tag{4.13}$$

In this context, the flexibility matrix $\mathbf{A}$ is the subspace flexibility matrix consisting of elements a_{ij} ($i = 1, 2, \ldots, r$; $j = 1, 2, \ldots, r$), while the mass matrix $\mathbf{M}$ is the subspace mass matrix consisting of non-zero diagonal elements m_{ii} ($i = 1, 2, \ldots, r$). The eigenvalues yielded from the individual subspaces are the actual eigenvalues of the original problem. Thus, instead of solving an nth-degree polynomial characteristic equation in λ for the n roots of λ (i.e. eigenvalues), we need only to solve, independently of each other, a series of lower degree characteristic equations in λ. In our example of the 16-node cable net, the decomposition results in the following independent characteristic equations in λ: two third-degree, two first-degree and one fourth-degree (the other fourth-degree equation being identical to this).

In this example, we have seen the usefulness of the group-theoretic approach in predicting not only the shape of vibration modes but also the number of modes of vibration of a given symmetry type. We have also seen its ability to predict the occurrence of degenerate modes (that is, modes of the same frequency of vibration), and to separate these for ease of computation. The latter are always associated with irreducible representations of dimension greater than one. The number of linearly independent modes of a particular frequency is simply given by the dimension of the corresponding irreducible representation. Now, the fifth irreducible representation of symmetry group C_{4v} (denoted by $R^{(5)}$) is two dimensional, so the corresponding subspace $S^{(5)}$ will always be associated with twice-repeating roots. Yet again, we see group theory shedding important insights into the properties of a system, even before actual calculations for natural frequencies and exact mode shapes are performed.

5. Layered space grids

(a) Symmetries of layered space grids

Figure 5 shows some symmetric configurations of typical double-layer space grids [14]. The upper diagram is the plan view of the grid, with nodes and relevant axes of symmetry labelled as shown. The lower diagram is a side view of the grid. The z-axis points in the upward vertical direction, while the h-axis lies in the horizontal plane of the bottom layer of nodes. The patterns of members, joints and supports all conform, with respect to size and type, to the overall symmetry of the configuration. Here, we assume that the grids are relatively shallow in relation to their horizontal dimensions (which is usually the case for long-span roofing applications), implying that the transverse stiffness of the grids is much lower than the in-plane (horizontal) stiffnesses in the two lateral directions. Thus, vertical motions dominate. Where this assumption is not valid, it is necessary to consider all three possible translational motions of the nodes of the space grid, typically the motions in the three Cartesian directions.

The triangular grid of figure 5*a* has 10 nodes in the lower layer (three of which are supported and not numbered in the diagram) and six nodes in the upper layer (whose positions in plan coincide with the centroids of six of the triangular panels of the lower layer), giving a total of 13 degrees of freedom corresponding to the small vertical motions of the 13 unsupported nodes. The total number of members making up the grid is 45 (18 in the lower layer, nine in the upper layer and 18 linking the two layers). The configuration has threefold rotational symmetry about the central vertical z-axis (which passes through node 4) and three reflection planes, giving it six symmetry elements forming the group C_{3v}.

The hexagonal grid of figure 5*b* has 19 nodes in the lower layer, six of which are supported (the corner nodes in the plan view). The upper layer has 24 nodes whose positions in plan coincide

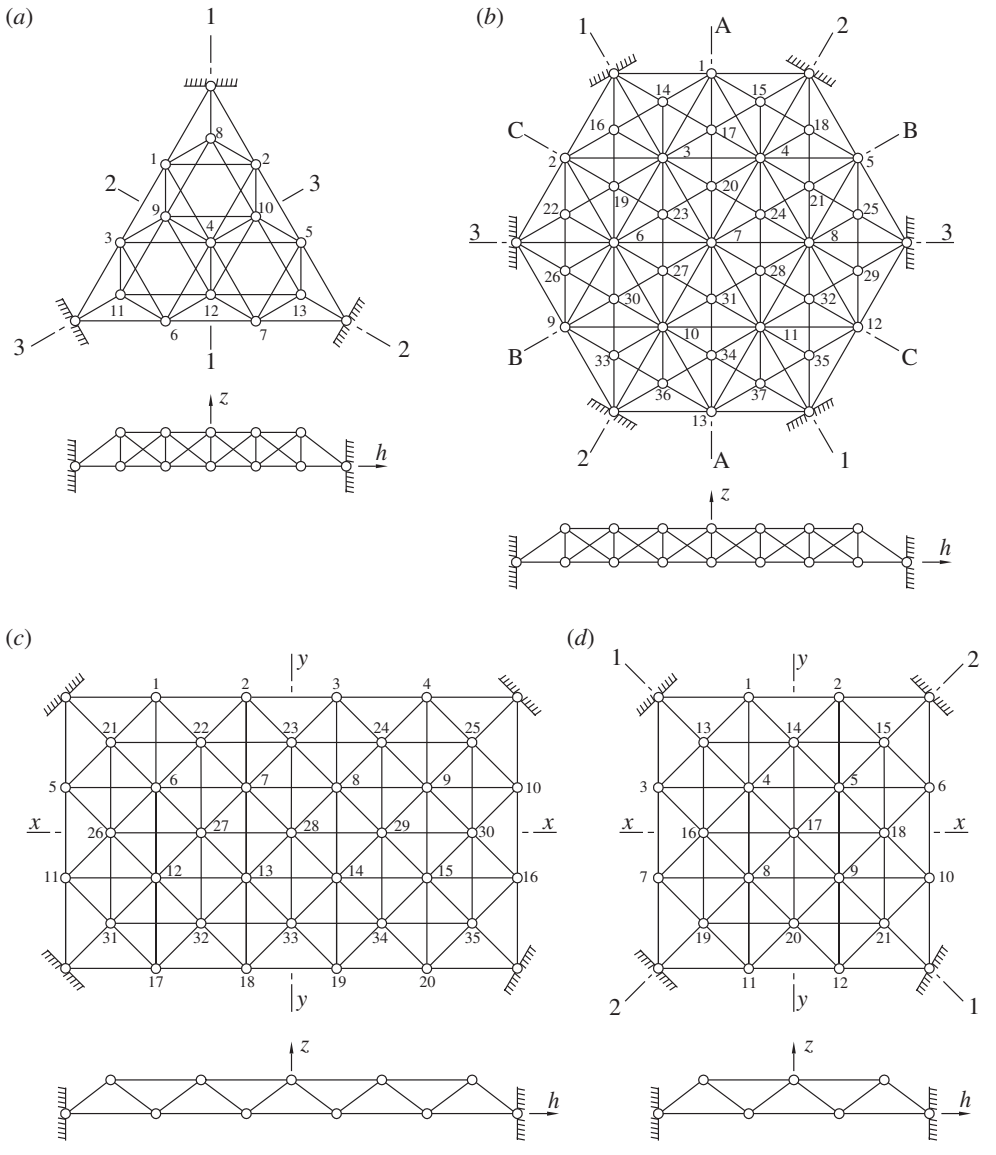

Figure 5. Double-layer space grids of various configurations: (*a*) triangular grid with C_{3v} symmetry; (*b*) hexagonal grid with C_{6v} symmetry; (*c*) rectangular grid with C_{2v} symmetry; and (*d*) square grid with C_{4v} symmetry.

with the centroids of the 24 triangular panels of the lower layer. There are therefore 37 degrees of freedom corresponding to the small vertical motions of the unsupported nodes. The total number of members may easily be seen to be 144. The symmetry possessed by the configuration comprises sixfold rotational symmetry about the *z*-axis (which passes through node 7), and six reflections, giving a total of 12 symmetry elements forming the group C_{6v}.

The rectangular and square grids of figure 5*c*,*d* are of the square-on-square offset configurations, with the panel sizes of the two layers being equal. The rectangular grid (figure 5*c*) has 35 free nodes (i.e. 35 degrees of freedom) interconnected by a total of 120 members. The square grid (figure 5*d*) has 21 free nodes and 72 members. The freedoms of interest are the small vertical motions of the unsupported nodes. Clearly, these configurations belong to symmetry groups C_{2v} and C_{4v}, respectively.

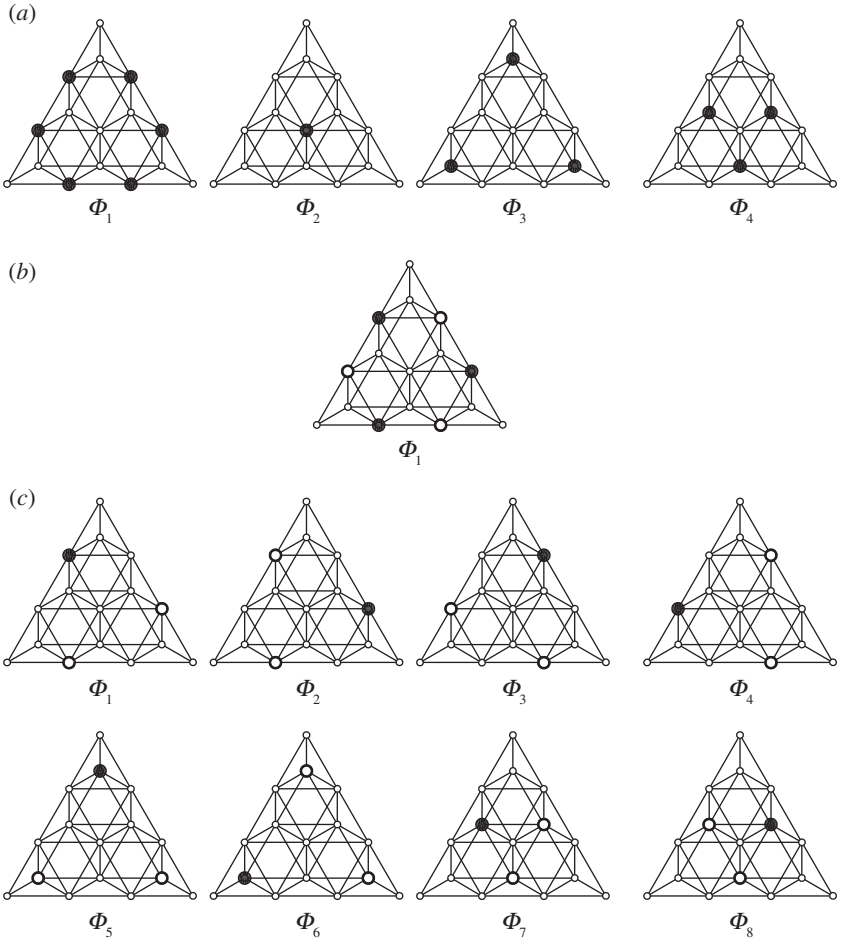

Figure 6. Triangular space grid: basis vectors of the subspaces: (*a*) subspace $S^{(1)}$; (*b*) subspace $S^{(2)}$; and (*c*) subspace $S^{(3)}$.

(b) Symmetry-adapted freedoms and vibration modes

Let the n degrees of freedom (corresponding to the small vertical motions of the n unsupported nodes) of the grid be denoted by $\{v_1, v_2, \ldots, v_n\}$, the numerical subscripts referring to the nodal numbering in the diagrams in figure 5. For a given problem, we apply in the usual manner an idempotent $P^{(i)}$ to each of the positions of the n degrees of freedom in turn, to generate a total of n symmetry-adapted freedoms, from which we can select a set of r_i *independent* symmetry-adapted freedoms as the *basis vectors* Φ_j $(j = 1, 2, \ldots, r_i)$ spanning the subspace.

For the triangular grid (symmetry group C_{3v}), the results show that subspaces $S^{(1)}$, $S^{(2)}$ and $S^{(3)}$ have 4, 1 and 8 basis vectors, respectively. Therefore, the system will have four modes of vibration (and corresponding four natural frequencies) with symmetry of type $S^{(1)}$, one mode of vibration of symmetry type $S^{(2)}$ and eight modes of vibration of symmetry type $S^{(3)}$, which all add up to the 13 degrees of freedom of the grid. The symmetries of the subspaces are evident when the basis vectors are plotted (figure 6). In these plots, the filled circles (black dots) denote downward movement of the nodes, whereas the open circles (rings) denote upward movement. With this knowledge, we may choose to compute the natural frequencies and mode shapes for modes of vibration of *selected symmetry*, without having to tackle the entire problem. Because the irreducible representation associated with the subspace $S^{(3)}$ is two dimensional [1], we expect the roots of the eigenvalue problem associated with subspace $S^{(3)}$ to be doubly repeating (i.e. only four distinct natural frequencies of vibration will need to be computed).

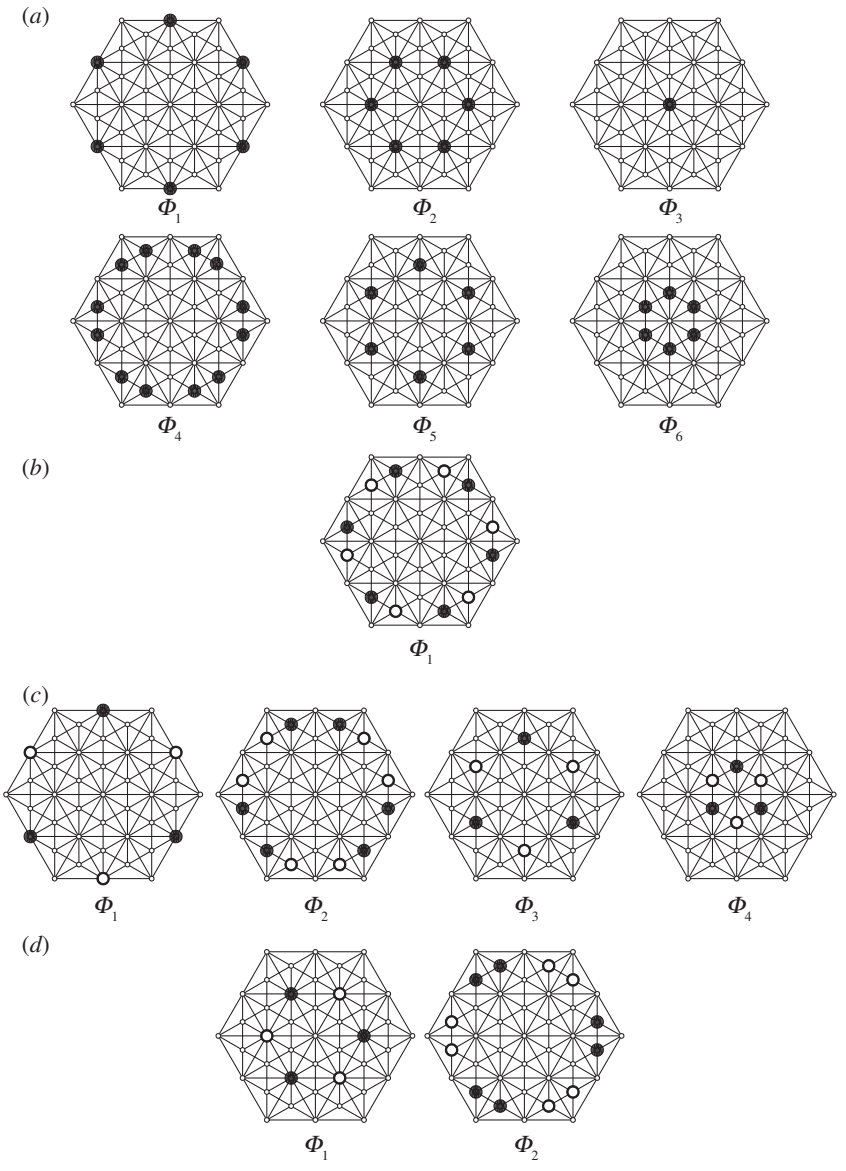

Figure 7. Hexagonal space grid: basis vectors of the first four subspaces: (*a*) subspace $S^{(1)}$; (*b*) subspace $S^{(2)}$; (*c*) subspace $S^{(3)}$; and (*d*) subspace $S^{(4)}$.

For the hexagonal grid (symmetry group C_{6v}), the subspaces $S^{(1)}, S^{(2)}, S^{(3)}, S^{(4)}, S^{(5)}$ and $S^{(6)}$ of the problem are found to be of dimensions 6, 1, 4, 2, 12 and 12, respectively. This system will therefore have six modes of vibration (and corresponding six natural frequencies) with symmetry of type $S^{(1)}$, one mode of vibration of symmetry type $S^{(2)}$, four modes of vibration of symmetry type $S^{(3)}$, two modes of vibration of symmetry type $S^{(4)}$, 12 modes of vibration of symmetry type $S^{(5)}$ and 12 modes of vibration of symmetry type $S^{(6)}$, which all add up to the 37 degrees of freedom of the grid. Figure 7 shows the plots of the basis vectors of the first four subspaces, allowing the symmetries of these to be visualized. The plots of the basis vectors of subspaces $S^{(5)}$ and $S^{(6)}$ have not been shown (there are too many), but we note that these last two subspaces are associated with two-dimensional irreducible representations. Therefore, only six distinct frequencies (not 12) will need to be computed for each subspace.

For the rectangular grid (symmetry group C_{2v}), we find that the subspaces $S^{(1)}, S^{(2)}, S^{(3)}$ and $S^{(4)}$ of the problem are of dimensions 11, 7, 9 and 8, respectively. The system will therefore have 11 modes of vibration (and corresponding 11 natural frequencies) with symmetry of type $S^{(1)}$, seven modes of vibration of symmetry type $S^{(2)}$, nine modes of vibration of symmetry type $S^{(3)}$ and eight modes of vibration of symmetry type $S^{(4)}$, which all add up to the 35 degrees of freedom of the grid.

For the square grid (symmetry group C_{4v}), the associated subspaces $S^{(1)}, S^{(2)}, S^{(3)}, S^{(4)}, S^{(5,1)}$ and $S^{(5,2)}$ are of dimensions 5, 1, 2, 3, 5 and 5, respectively. The system will therefore have five modes of vibration (and corresponding five natural frequencies) with symmetry of type $S^{(1)}$, one mode of vibration of symmetry type $S^{(2)}$, two modes of vibration of symmetry type $S^{(3)}$, three modes of vibration of symmetry type $S^{(4)}$ and 10 modes of vibration of symmetry type $S^{(5)}$, which all add up to the 21 degrees of freedom of the grid. We further predict that subspace $S^{(5)}$, being associated with a two-dimensional irreducible representation, will feature doubly repeating roots (i.e. only five distinct eigenvalues), and consideration of either subspace $S^{(5,1)}$ or subspace $S^{(5,2)}$ will generate the five distinct eigenvalues or natural frequencies.

6. Thin elastic plates

(a) Governing equation of motion

The equation of motion for the undamped free vibration of a plate may be written as [34]

$$\frac{\partial^4 w}{\partial x^4} + 2\frac{\partial^4 w}{\partial x^2\,\partial y^2} + \frac{\partial^4 w}{\partial y^4} + \frac{\rho}{D}\frac{\partial^2 w}{\partial t^2} = 0, \tag{6.1}$$

where w is the transverse displacement at a point defined by the coordinates $\{x, y\}$ at any given time t, D is the flexural rigidity of the plate and ρ is the mass of the plate per unit area of its surface. Assuming harmonic vibration, we may write

$$w(x, y, t) = W(x, y)\sin\omega t, \tag{6.2}$$

where $W(x, y)$ is a shape function satisfying the boundary conditions and describing the shape of the deflected middle surface of the vibrating plate, and ω is a natural circular frequency of the plate. Substituting for w in equation (6.1), we obtain

$$\frac{\partial^4 W}{\partial x^4} + 2\frac{\partial^4 W}{\partial x^2\,\partial y^2} + \frac{\partial^4 W}{\partial y^4} - \eta W = 0, \tag{6.3}$$

where

$$\eta = \frac{\rho\omega^2}{D}. \tag{6.4}$$

The ordinary finite-difference representation of equation (6.3) at a pivotal point (m, n) of the mesh, based on central differences and taking equal mesh intervals $d = \Delta x = \Delta y$ (in the x and y directions), is as follows [34]:

$$\begin{aligned} &20W_{m,n} - 8(W_{m-1,n} + W_{m+1,n} + W_{m,n-1} + W_{m,n+1}) \\ &\quad + 2(W_{m-1,n-1} + W_{m-1,n+1} + W_{m+1,n-1} + W_{m+1,n+1}) \\ &\quad + W_{m-2,n} + W_{m+2,n} + W_{m,n-2} + W_{m,n+2} - \lambda W_{m,n} = 0, \end{aligned} \tag{6.5}$$

where

$$\lambda = \eta d^4. \tag{6.6}$$

Figure 8 shows a rectangular plate simply supported on all four edges, with an equispaced grid of mesh lines in the x and y directions giving a total of 24 mesh points on the plate. Here, we have chosen to adopt a relatively coarse mesh in order to permit the relevant group-theoretic calculations to be performed in a manageable manner (the systems of equations needing to be solved will not be too large), which also makes it easy for the reader to follow the steps. This mesh

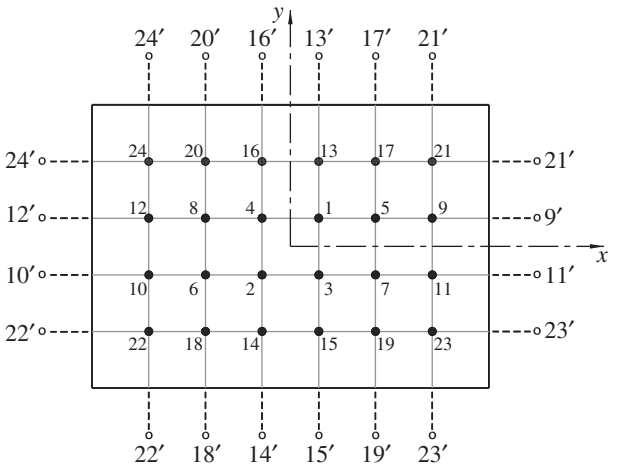

Figure 8. Rectangular plate simply supported along all four edges and divided into a square mesh with 24 mesh points.

is adequate for the purposes of bringing out the key attributes of the group-theoretic procedure, but clearly if a higher degree of accuracy in the numerical values is required, then a finer mesh ought to be adopted. The mesh configuration conforms to symmetry group C_{2v}. Mesh points have been numbered in accordance with group-theoretic rules [28]. Also shown outside the boundary of the plate (as mirror images of the adjacent nodes on the plate) are the relevant fictitious nodes, for use in the finite-difference equations for the real nodes.

(b) Basis vectors

Applying the idempotents $P^{(1)}, P^{(2)}, P^{(3)}$ and $P^{(4)}$ of symmetry group C_{2v} (equations (2.1)), for subspaces $S^{(1)}, S^{(2)}, S^{(3)}$ and $S^{(4)}$, respectively, to each of the 24 nodal functions $\phi_1, \phi_2, \ldots, \phi_{24}$ associated with the mesh points of the plate, we obtain 24 linear combinations of these functions for each subspace, not all of which are independent. Selecting a set of independent combinations of functions as the basis vectors for the subspace in question, we find that all four subspaces are six dimensional (i.e. have six basis vectors each). The sets of basis vectors $\Phi_j^{(i)}$ for all four subspaces ($i = 1, 2, 3, 4$; $j = 1, 2, 3, 4, 5, 6$) may be collected together as follows:

$$\begin{bmatrix} \Phi_1^{(1)} & \Phi_2^{(1)} & \Phi_3^{(1)} & \Phi_4^{(1)} & \Phi_5^{(1)} & \Phi_6^{(1)} \\ \Phi_1^{(2)} & \Phi_2^{(2)} & \Phi_3^{(2)} & \Phi_4^{(2)} & \Phi_5^{(2)} & \Phi_6^{(2)} \\ \Phi_1^{(3)} & \Phi_2^{(3)} & \Phi_3^{(3)} & \Phi_4^{(3)} & \Phi_5^{(3)} & \Phi_6^{(3)} \\ \Phi_1^{(4)} & \Phi_2^{(4)} & \Phi_3^{(4)} & \Phi_4^{(4)} & \Phi_5^{(4)} & \Phi_6^{(4)} \end{bmatrix}$$
$$= \begin{bmatrix} 1 & 1 & 1 & 1 \\ 1 & 1 & -1 & -1 \\ 1 & -1 & 1 & -1 \\ 1 & -1 & -1 & 1 \end{bmatrix} \begin{bmatrix} \phi_1 & \phi_5 & \phi_9 & \phi_{13} & \phi_{17} & \phi_{21} \\ \phi_2 & \phi_6 & \phi_{10} & \phi_{14} & \phi_{18} & \phi_{22} \\ \phi_3 & \phi_7 & \phi_{11} & \phi_{15} & \phi_{19} & \phi_{23} \\ \phi_4 & \phi_8 & \phi_{12} & \phi_{16} & \phi_{20} & \phi_{24} \end{bmatrix}. \tag{6.7}$$

The symmetry types associated with the four subspaces of this problem may be visualized by reference to figure 9, in which the sixth basis vector of each subspace $\Phi_6^{(i)}$ ($i = 1, 2, 3, 4$) has been plotted. As all basis vectors of a given subspace have the same symmetry type, there is no point in plotting all of them in order to illustrate the symmetry; one suffices.

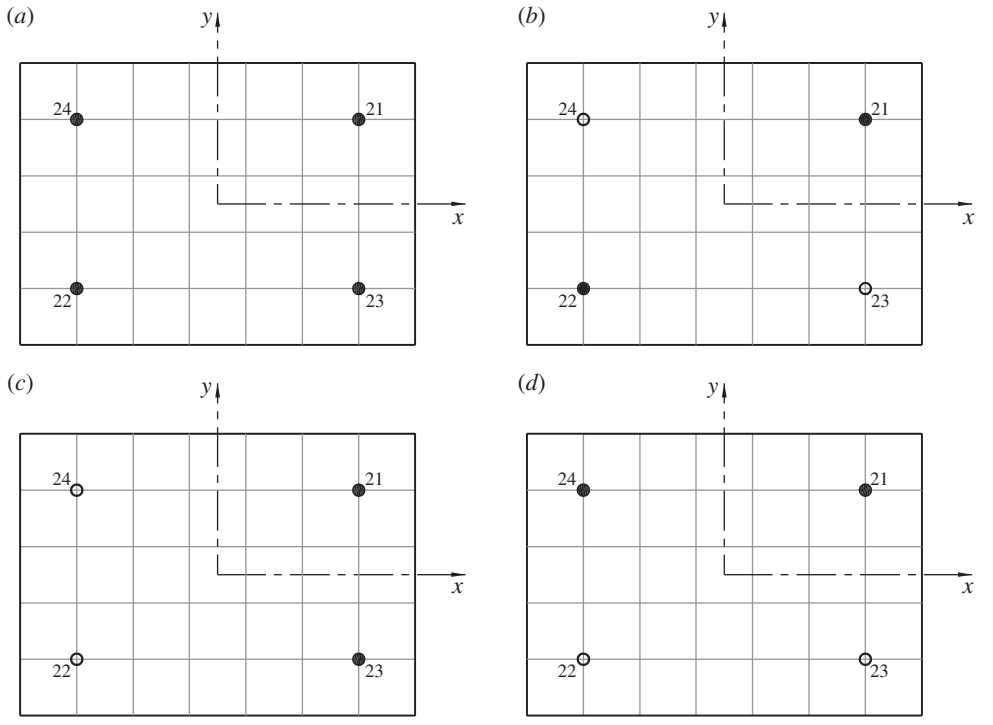

Figure 9. Rectangular plate: symmetry types of the four subspaces illustrated by the sixth basis vector of each subspace: (*a*) $\Phi_6^{(1)}$ of subspace $S^{(1)}$; (*b*) $\Phi_6^{(2)}$ of subspace $S^{(2)}$; (*c*) $\Phi_6^{(3)}$ of subspace $S^{(3)}$; and (*d*) $\Phi_6^{(4)}$ of subspace $S^{(4)}$. Filled (black) circles denote positive coordinates of the basis vectors, while open circles (rings) denote negative coordinates.

(c) Conventional finite-difference equations

In the group-theoretic formulation developed by Zingoni [28], we do not need to write down the finite-difference equations for all the nodes of the mesh, and then operate on these to reduce the number of equations. *Instead, we need only write down the finite-difference equations for the nodes corresponding to the first components of the basis vectors of each subspace and operate on this reduced set of equations in order to generate all the required symmetry-adapted finite-difference equations for the various subspaces of the problem*. For our example, the set of nodes for which finite-difference equations need to be written down is $\{1, 5, 9, 13, 17, 21\}$.

All edges are simply supported, implying that $W = 0$ for all nodes lying on the edges of the plate. For the fictitious nodes of the finite-difference mesh (figure 8), the deflections W are equal in magnitude but opposite in sign to those of the corresponding real nodes. The central finite-difference equations for nodes $\{1, 5, 9, 13, 17, 21\}$ (in that order) become

$$(20-\lambda)W_1 + 2W_2 - 8W_3 - 8W_4 - 8W_5 + 2W_7 + W_8 + W_9 - 8W_{13} + W_{15} + 2W_{16} + 2W_{17} = 0, \tag{6.8a}$$

$$-8W_1 + 2W_3 + W_4 + (20-\lambda)W_5 - 8W_7 - 8W_9 + 2W_{11} + 2W_{13} - 8W_{17} + W_{19} + 2W_{21} = 0, \tag{6.8b}$$

$$W_1 - 8W_5 + 2W_7 + (19-\lambda)W_9 - 8W_{11} + 2W_{17} - 8W_{21} + W_{23} = 0, \tag{6.8c}$$

$$-8W_1 + W_3 + 2W_4 + 2W_5 + (19-\lambda)W_{13} - 8W_{16} - 8W_{17} + W_{20} + W_{21} = 0, \tag{6.8d}$$

$$2W_1 - 8W_5 + W_7 + 2W_9 - 8W_{13} + W_{16} + (19-\lambda)W_{17} - 8W_{21} = 0 \tag{6.8e}$$

and

$$2W_5 - 8W_9 + W_{11} + W_{13} - 8W_{17} + (18-\lambda)W_{21} = 0. \tag{6.8f}$$

(d) Symmetry-adapted finite-difference equations and system eigenvalues

For any given basis vector $\Phi_j^{(i)}$ of subspace $S^{(i)}$, the coefficients of the components ϕ are either $+1$ or -1 for all subspaces. These coefficients give the relative values of the transverse displacements associated with the nodes of Φ_j. For a given r-dimensional subspace, we will denote the amplitude of the displacements associated with the nodes of Φ_j ($j = 1, 2, \ldots, r$) by the parameter f_j. This amplitude will be the same for all nodes of Φ_j. This formulation results in an r-dimensional eigenvalue problem within the subspace $S^{(i)}$, which upon solving yields the r eigenvalues (natural circular frequencies) for that subspace. As stated earlier, these subspace eigenvalues are also eigenvalues of the full space of the problem, and no further computations are required. Consider subspace $S^{(1)}$. From the coefficients of $\Phi_j^{(1)}$ ($j = 1, 2, \ldots, 6$), let

$$W_1 = W_2 = W_3 = W_4 = f_1, \tag{6.9a}$$

$$W_5 = W_6 = W_7 = W_8 = f_2, \tag{6.9b}$$

$$W_9 = W_{10} = W_{11} = W_{12} = f_3, \tag{6.9c}$$

$$W_{13} = W_{14} = W_{15} = W_{16} = f_4, \tag{6.9d}$$

$$W_{17} = W_{18} = W_{19} = W_{20} = f_5 \tag{6.9e}$$

and

$$W_{21} = W_{22} = W_{23} = W_{24} = f_6. \tag{6.9f}$$

Making the above substitutions into each of equations (6.8), we obtain six equations in $\{f_1, f_2, f_3, f_4, f_5, f_6\}$:

$$\begin{bmatrix} (6-\lambda) & -5 & 1 & -5 & 2 & 0 \\ -5 & (12-\lambda) & -6 & 2 & -7 & 2 \\ 1 & -6 & (11-\lambda) & 0 & 2 & -7 \\ -5 & 2 & 0 & (11-\lambda) & -7 & 1 \\ 2 & -7 & 2 & -7 & (19-\lambda) & -8 \\ 0 & 2 & -7 & 1 & -8 & (18-\lambda) \end{bmatrix} \begin{bmatrix} f_1 \\ f_2 \\ f_3 \\ f_4 \\ f_5 \\ f_6 \end{bmatrix} = \begin{bmatrix} 0 \\ 0 \\ 0 \\ 0 \\ 0 \\ 0 \end{bmatrix}. \tag{6.10}$$

The vanishing condition for the determinant of the above 6×6 matrix yields a sixth-degree polynomial equation in λ, whose roots (the required eigenvalues) are obtained as

$$\lambda_1 = 0.336;\ \lambda_2 = 3.752;\ \lambda_3 = 7.930;\ \lambda_4 = 13.169;\ \lambda_5 = 17.414;\ \text{and}\ \lambda_6 = 34.398.$$

Considering subspace $S^{(2)}$ next, from the coefficients of the $\Phi_j^{(2)}$ ($j = 1, 2, \ldots, 6$), let

$$W_1 = W_2 = -W_3 = -W_4 = f_1, \tag{6.11a}$$

$$W_5 = W_6 = -W_7 = -W_8 = f_2, \tag{6.11b}$$

$$W_9 = W_{10} = -W_{11} = -W_{12} = f_3, \tag{6.11c}$$

$$W_{13} = W_{14} = -W_{15} = -W_{16} = f_4, \tag{6.11d}$$

$$W_{17} = W_{18} = -W_{19} = -W_{20} = f_5 \tag{6.11e}$$

and

$$W_{21} = W_{22} = -W_{23} = -W_{24} = f_6. \tag{6.11f}$$

Making the above substitutions into each of equations (6.8), we obtain

$$\begin{bmatrix} (38-\lambda) & -11 & 1 & -11 & 2 & 0 \\ -11 & (28-\lambda) & -10 & 2 & -9 & 2 \\ 1 & -10 & (27-\lambda) & 0 & 2 & -9 \\ -11 & 2 & 0 & (27-\lambda) & -9 & 1 \\ 2 & -9 & 2 & -9 & (19-\lambda) & -8 \\ 0 & 2 & -9 & 1 & -8 & (18-\lambda) \end{bmatrix} \begin{bmatrix} f_1 \\ f_2 \\ f_3 \\ f_4 \\ f_5 \\ f_6 \end{bmatrix} = \begin{bmatrix} 0 \\ 0 \\ 0 \\ 0 \\ 0 \\ 0 \end{bmatrix}, \tag{6.12}$$

Table 3. Natural circular frequencies ω (in rad s^{-1}) for the rectangular plate.

subspace $S^{(1)}$	subspace $S^{(2)}$	subspace $S^{(3)}$	subspace $S^{(4)}$
(1) 22.20[a]	(5) 81.73[a]	(2) 43.45[a]	(3) 60.48[a]
(4) 74.15[a]	(12) 146.50	(7) 108.22	(8) 112.43
(6) 107.80	(15) 167.33	(9) 129.05	(11) 146.09
(10) 138.92	(19) 198.45	(14) 160.16	(16) 177.20
(13) 159.74	(21) 232.10	(17) 193.82	(18) 198.02
(20) 224.52	(24) 284.05	(22) 245.77	(23) 262.80

[a]First five modes.

leading to the results

$$\lambda_1 = 4.558;\ \lambda_2 = 14.646;\ \lambda_3 = 19.106;\ \lambda_4 = 26.873;\ \lambda_5 = 36.761;\ \text{and}\ \lambda_6 = 55.056.$$

Proceeding in the same way for the remaining two subspaces, we obtain the results

Subspace $S^{(3)}$

$$\lambda_1 = 1.288;\ \lambda_2 = 7.992;\ \lambda_3 = 11.364;\ \lambda_4 = 17.505;\ \lambda_5 = 25.635;\ \text{and}\ \lambda_6 = 41.216.$$

Subspace $S^{(4)}$

$$\lambda_1 = 2.496;\ \lambda_2 = 8.626;\ \lambda_3 = 14.563;\ \lambda_4 = 21.427;\ \lambda_5 = 26.760;\ \text{and}\ \lambda_6 = 47.128.$$

(e) Numerical results

Natural circular frequencies were evaluated for a rectangular steel plate of dimensions 7 m × 5 m, assuming all edges are simply supported [28]. The thickness h of the plate was given as 25 mm. The density γ of the steel was taken as 7800 kg m^{-3}, the modulus of elasticity E as 200×10^9 N m^{-2} and Poisson's ratio ν as 0.3. Table 3 shows values of ω obtained on the basis of a finite-difference mesh of spacing 1 m × 1 m in the x and y directions. The numbers in brackets (*mode numbers*) denote the ascending order of the frequencies, from 1 up to 24.

From the results, we observe yet another attribute of the group-theoretic formulation. Apart from the property of breaking up the original problem into smaller problems which are much easier to solve, we see that the group-theoretic decomposition also separates modes whose frequencies are very close to each other, eliminating the numerical problems usually associated with the computation of frequencies that are nearly coincident. For instance, modes 6, 7 and 8 have closely spaced circular frequencies of {107.80; 108.22; 112.43} rad s^{-1}, respectively, but these frequencies are extracted separately within subspaces $S^{(1)}$, $S^{(3)}$ and $S^{(4)}$.

7. Concluding remarks

In this paper, we have shown how the group-theoretic procedure, besides its more obvious merits of reducing computational effort, affords useful insights into the vibration properties of a structural system without the necessity of first performing detailed numerical computations. Such qualitative benefits have included a prior appreciation of all the possible symmetries of the modes of vibration, the prediction of the number of modes of a given symmetry type, the identification of modes associated with the same frequencies, the prediction of nodal lines and stationary points of a vibrating system, and the untangling of clustered frequencies.

Information of this type greatly helps in understanding why certain phenomena occur in particular physical systems, depending on the types of symmetries they possess. In turn, this allows us to design structural systems to be less susceptible to detrimental phenomena, for example resonance. It is believed that group theory has the potential to reveal new as yet

undiscovered phenomena with regard to the static, kinematic, stability and dynamic behaviour of complex structural systems which are rich in symmetry.

Acknowledgements. I thank Mr A. Rule of the University of Cape Town for assistance with the preparation of the illustrations.

Funding statement. I thank the National Research Foundation of South Africa for the financial support.

References

1. Hamermesh M. 1962 *Group theory and its application to physical problems*. Oxford, UK: Pergamon Press.
2. Schonland D. 1965 *Molecular symmetry*. London, UK: Van Nostrand.
3. Weyl H. 1932 *Theory of groups and quantum mechanics*. New York, NY: Dover Publications.
4. Wigner EP. 1959 *Group theory and its applications to the quantum mechanics of atomic spectra*. New York, NY: Academic Press.
5. Sattinger DH. 1979 *Group theoretic methods in bifurcation theory*. Lecture Notes in Mathematics no. 762. Berlin, Germany: Springer.
6. Werner B, Spence A. 1984 The computation of symmetry-breaking bifurcation points. *SIAM J. Numer. Anal.* **21**, 388–399. (doi:10.1137/0721029)
7. Healey TJ. 1988 A group-theoretic approach to computational bifurcation problems with symmetry. *Comput. Methods Appl. Mech. Eng.* **67**, 257–295. (doi:10.1016/0045-7825(88)90049-7)
8. Dellnitz M, Werner B. 1989 Computational methods for bifurcation problems with symmetries, with special attention to steady-state and Hopf bifurcation points. *J. Comput. Appl. Math.* **26**, 97–123. (doi:10.1016/0377-0427(89)90150-7)
9. Zlokovic GM. 1989 *Group theory and G-vector spaces in structural analysis*. Chichester, UK: Ellis Horwood.
10. Healey TJ, Treacy JA. 1991 Exact block diagonalisation of large eigenvalue problems for structures with symmetry. *Int. J. Numer. Methods Eng.* **31**, 265–285. (doi:10.1002/nme.1620310205)
11. Zingoni A. 1996 An efficient computational scheme for the vibration analysis of high-tension cable nets. *J. Sound Vib.* **189**, 55–79. (doi:10.1006/jsvi.1996.0005)
12. Mohan SJ, Pratap R. 2002 A group theoretic approach to the linear free vibration analysis of shells with dihedral symmetry. *J. Sound Vib.* **252**, 317–341. (doi:10.1006/jsvi.2001.4042)
13. Mohan SJ, Pratap R. 2004 A natural classification of vibration modes of polygonal ducts based on group theoretic analysis. *J. Sound Vib.* **269**, 745–764. (doi:10.1016/S0022-460X(03)00129-9)
14. Zingoni A. 2005 On the symmetries and vibration modes of layered space grids. *Eng. Struct.* **27**, 629–638. (doi:10.1016/j.engstruct.2004.12.004)
15. Kaveh A, Nikbakht M. 2007 Decomposition of symmetric mass–spring vibrating systems using groups, graphs and linear algebra. *Commun. Numer. Methods Eng.* **23**, 639–664. (doi:10.1002/cnm.913)
16. Zingoni A. 2008 On group-theoretic computation of natural frequencies for spring–mass dynamic systems with rectilinear motion. *Commun. Numer. Methods Eng.* **24**, 973–987. (doi:10.1002/cnm.1003)
17. Kaveh A, Nikbakht M. 2010 Improved group-theoretical method for eigenvalue problems of special symmetric structures using graph theory. *Adv. Eng. Softw.* **41**, 22–31. (doi:10.1016/j.advengsoft.2008.12.003)
18. Zingoni A, Pavlovic MN, Zlokovic GM. 1995 A symmetry-adapted flexibility approach for multi-storey space frames: general outline and symmetry-adapted redundants. *Struct. Eng. Rev.* **7**, 107–119.
19. Zingoni A, Pavlovic MN, Zlokovic GM. 1995 A symmetry-adapted flexibility approach for multi-storey space frames: symmetry-adapted loads. *Struct. Eng. Rev.* **7**, 121–130.
20. Kangwai RD, Guest SD, Pellegrino S. 1999 An introduction to the analysis of symmetric structures. *Comput. Struct.* **71**, 671–688. (doi:10.1016/S0045-7949(98)00234-X)
21. Kangwai RD, Guest SD. 1999 Detection of finite mechanisms in symmetric structures. *Int. J. Solids Struct.* **36**, 5507–5527. (doi:10.1016/S0020-7683(98)00234-0)
22. Kangwai RD, Guest SD. 2000 Symmetry-adapted equilibrium matrices. *Int. J. Solids Struct.* **37**, 1525–1548. (doi:10.1016/S0020-7683(98)00318-7)
23. Zlokovic GM. 1992 *Group supermatrices in finite element analysis*. Chichester, UK: Ellis Horwood.

24. Wohlever JC. 1999 Some computational aspects of a group theoretic finite element approach to the buckling and postbuckling analyses of plates and shells-of-revolution. *Comput. Methods Appl. Mech. Eng.* **170**, 373–406. (doi:10.1016/S0045-7825(98)00204-7)
25. Zingoni A. 2005 A group-theoretic formulation for symmetric finite elements. *Finite Elem. Anal. Des.* **41**, 615–635. (doi:10.1016/j.finel.2004.10.004)
26. Zlokovic G, Maneski T, Nestorovic M. 2004 Group theoretical formulation of quadrilateral and hexahedral isoparametric finite elements. *Comput. Struct.* **82**, 883–899. (doi:10.1016/j.compstruc.2004.02.017)
27. Kaveh A, Fazli H. 2007 Graph coloration and group theory in dynamic analysis of symmetric finite element models. *Finite Elem. Anal. Des.* **43**, 901–911. (doi:10.1016/j.finel.2007.06.002)
28. Zingoni A. 2012 A group-theoretic finite-difference formulation for plate eigenvalue problems. *Comput. Struct.* **112/113**, 266–282. (doi:10.1016/j.compstruc.2012.08.009)
29. Zingoni A. 2012 Symmetry recognition in group-theoretic computational schemes for complex structural systems. *Comput. Struct.* **94/95**, 34–44. (doi:10.1016/j.compstruc.2011.12.004)
30. Zingoni A. 2009 Group-theoretic exploitations of symmetry in computational solid and structural mechanics. *Int. J. Numer. Methods Eng.* **79**, 253–289. (doi:10.1002/nme.2576)
31. Ikeda K, Murota K, Fujii H. 1991 Bifurcation hierarchy of symmetric structures. *Int. J. Solids Struct.* **27**, 1551–1573. (doi:10.1016/0020-7683(91)90077-S)
32. Ikeda K, Murota K. 1991 Bifurcation analysis of symmetric structures using block-diagonalisation. *Comput. Methods Appl. Mech. Eng.* **86**, 215–243. (doi:10.1016/0045-7825(91)90128-S)
33. Wohlever JC, Healey TJ. 1995 A group-theoretic approach to the global bifurcation analysis of an axially compressed cylindrical shell. *Comput. Methods Appl. Mech. Eng.* **122**, 315–349. (doi:10.1016/0045-7825(94)00734-5)
34. Szilard R. 1974 *Theory and analysis of plates: classical and numerical methods*. Englewood Cliffs, NJ: Prentice-Hall.